# A COMPARISON OF OBJECTED-ORIENTED AND PIXEL-BASED CLASSIFICATION METHODS FOR FUEL TYPE MAP USING HYPERION IMAGERY

Yeosang Yoon and Yongseung Kim

Remote Sensing Department, Korea Aerospace Research Institute
45 Eoeun-Dong, Youseong-Gu, Daejeon 305-333, Korea
Tel: (82)-42-860-2276 Fax: (82)-42-860-2605
E-mail: gise@kari.re.kr, yskim@kari.re.kr

**ABSTRACT:** The knowledge of fuel load and composition is important for planning and managing the fire hazard and risk. However, fuel mapping is extremely difficult because fuel properties vary at spatial scales, change depending on the seasonal situations and are affected by the surrounding environment. Remote sensing has potential of reduction the uncertainty in mapping fuels and offers the best approach for improving our abilities. This paper compared the results of object-oriented classification to a pixel-based classification for fuel type map derived from Hyperion hyperspectral data that could be enable to provide this information and allow a differentiation of material due to their typical spectra. Our methodological approach for fuel type map is characterized by the result of the spectral mixture analysis (SMA) that can used to model the spectral variability in multi- or hyperspectral images and to relate the results to the physical abundance of surface constitutes represented by the spectral endmembers. Object-oriented approach was based on segment based endmember selection, while pixel-based method used standard SMA. To validate and compare, we used true-color high resolution orthoimagery

**KEY WORDS:** object-oriented, spectral mixture analysis, fuel type, endmember selection

## 1. INTRODUCTION

Wildland fuels are critical elements in many wildland fire planning and management activities. Fire fuels are a particular significance to natural resource managers because unlikely weather and topography, humans can change the available quantities of fuels (Keane *et al.*, 2001). Remote sensing has the potential to reduce uncertainty when assessing fuel fuels and offers the best approach for improving our abilities to assess spatially and temporally varying fuel characteristics (Roberts and Dennision, 1999).

In Korea Peninsula, the spring season climate which is dry weather results in water deficits and ecosystems that are highly sensitive to climate perturbations. Spring drought coupled with the presence of shrub and forested community makes wildfire that is one of the most serious economic and life-threatening natural disasters in the regions. According to the National Emergency Management Agency statistics, about 60 percent of all wildfire broke out in spring time with a great deal of damage to the areas.

Fuels are defined as the physical characteristics, such as loading (weight per unit area), size (particle diameter), and bulk density (weight per unit volume) of the live and dead biomass that contribute to the spread, intensity, and severity of wildland fire (Keane *et al.*, 2001). The main criterion of classification is the propagation element, divided into three major groups: grass, shrub, or ground litter. In object-oriented classification, which is the technique that was adopted in this work, not only the spectral signature but also some spatial characteristics such as shape, texture, and neighbouring object were taken as the main classification factors (Kettig and Landgrebe, 1976; van der Sande *et al.*, 2003).

In this study, we analyzed and compared the results of object-oriented and pixel-based classification for fuel type using Hyperion, an imaging spectrometer on the Earth Observation 1(EO-1) satellite platform. For classification, we used spectral mixture analysis (SMA).

## 2. BACKGROUND

In the most extreme conditions, such as strong winds, high temperature and very low humidity, fire will burn across land with very low fuel fuels. However, the effects of fuels on fire behaviour will differ, depending on type and structure of the vegetation, the level of moisture in the fuel, the arrangement of the fuel, and the terrain (Roberts *et al.*, 2003; Rolf *et al.*, 2005). Therefore, there is a clear management advantage to have an understanding of fuel continuity across the landscape, especially for wildfire suppression planning. Historically, remote sensing has been more concern with mapping fire danger. High resolution and temporal variability imageries are usually used because of representing one of the greatest sources of uncertainty in predicting fire danger. In some case, fire danger is assessed using broadband sensor such as the Advanced Very High Resolution Radiometer (AVHRR), and Thematic Mapper (TM), through some combination of fuel type mapping, meteorology and ancillary geographic information

(Chuvieco and Salas, 1996). Roberts *et al.* and Dennison *et al.* describe new measures of fuel properties derived from hyperspectral system such as AVIRIS.

SMA technique assumes that the remotely sensed surface reflectance can be modeled as the linear combination of endmember reflectance spectra (Smith *et al.*, 1990). Endmember spectra (i.e., laboratory, reference, or image pixel spectra) are selected to represent the physical scene components of interest, but they also must adequately explain the majority of scene spectral variance. SMA proceeds with the formation of the following system of equations for each pixel in the image:

$$R_{mix,b} = \sum (f_{em} R_{em,b}) + \varepsilon_b \quad and \quad \sum f_{em} = 1 \qquad (1)$$

where $R_{mix,b}$ is reflectance of observed image spectrum at each band; $f_{em}$ is fraction of each endmember in observed mixed spectrum; $R_{em,b}$ is reflectance of each endmember at each band; $\varepsilon_b$ is band residual.

## 3. METHOD

### 3.1 Study Site

The study site is located in southwest part of GyeongGi-Do, Korea. This area consists of forest, farmland and small village. Although many species of trees are present, only a few species dominate the landscape including pine and oak.

### 3.2 Data

For our study, we used part of the Hyperion imagery acquired at approximately 02:00 UTC on April 3, 2002. Hyperion is a hyperspectral instrument on the Earth Observing 1 (EO-1) spacecraft that was launched on November 21, 2000. Hyperion imagery consists of 242 channels ranging from 356-2577nm, sampled approximately at a 10nm sampling interval. It is part of EO-1 platform and follows Landsat Enhanced Thematic Mapper (ETM) in its orbits, providing nearly simultaneous coverage. Each image contains data for a 7.65km wide (cross-track) by 185km long (along-track) region.

### 3.3 Image Analysis

In order to compare the information provided the object-oriented and pixel-based classification, all the necessary corrections in both images were made, and the same standardization was used but in a modified form according to the characteristics of the methodology (Figure 1).

**3.3.1 Detection and Correction of Abnormal Pixels:** Hyperion acquires data in pushbroom mode with two spectrometers, one in the visible and near infrared (VNIR) range and another in the short-wave infrared (SWIR) range. We used Hyperion data set is called Hyperion level 1b, which is radiometrically-corrected all bad pixels. However, bad pixels are still evident. In addition, there are dark vertical stripes in the image (Han *et al.*, 2002). In order to correct the abnormal pixels, we applied modified 3×3 average Filter to atypical pixels.

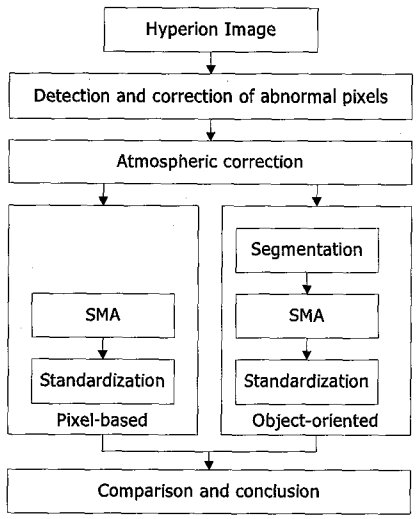

Figure 1. An overview of the methodology approach

**3.3.2 Atmospheric correction:** The Hyperion data was radiometrically corrected to reflectance using the FLAASH (Fast Line of sight Atmospheric Analysis of Hyperspectral Cubes) ver. 4.2. The surface reflectance was determined by the following equation:

$$L = \left(\frac{A\rho}{1-\rho_e S}\right) + \left(\frac{B\rho_e}{1-\rho_e S}\right) + L_a \qquad (2)$$

where $\rho$ is the pixel surface reflectance; $\rho_e$ is an average surface reflectance for the pixel; $S$ is the spherical albedo of the atmosphere; $L_a$ is the radiance back scattered by the atmosphere; $A$ and $B$ are coefficients that depend on atmospheric and geometric condition but not on the surface.

**3.3.3 Standardization:** The "Prometheus" system is based mainly on the type and height of the propagation element and it comprise the seven fuel types to be identified. However, it is not always possible to recognize all these classes in their exact form. Thus, for the Hyperion image and acquisition date, the following classes were used:

**Type 1:** no vegetation (bare soil > 60%, impervious > 60%, water/shadow > 60%)
**Type 2:** low shrubs or agricultural land (NPV < 20%, agricultural land > 30%)
**Type 3:** medium dead surface fuel (NPV > 30%)
**Type 4:** high dead surface fuel and broadleaved tree (NPV> 60%)
**Type 5**: Coniferous forest (GV > 60%)

**3.3.4 Pixel-based Classification:** SMA was used to map green vegetation (GV), non-photosynthetic vegetation (dead herbaceous plants, litter, and wood), bare soil,

shadow, agricultural land, and impervious (building, asphalt road, etc.). In SMA, The endmembers were selected from pure pixels with reference to the field spectrometer (GER3700) and high resolution orthoimagery and based on whether they are physically reasonable (fractions are between 0% and 100%) and meet criteria based on the overall fit and residuals.

**3.3.5 Object-oriented Classification:** The object-oriented approach first involved the segmentation of image data into objects. The image was segmented into object primitives or segments using eCognition. The segmentation of the image into object primitives was influenced by three parameters: scale, color, and shape. SMA method was also used for fuel types.

## 4. RESULTS/DISCUSSION

### 4.1 Detection and Correction of Abnormal pixels

There are many possible causes for the abnormal pixels including detector failure, errors during data transfer, and improper data correction. We corrected the abnormal pixels and removed atypical bands. Finally, we used 150 bands of 242 bands.

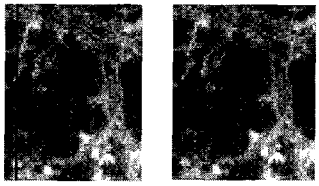

(a) Before (b) After
Figure 2. Abnormal pixel correction

### 4.2 Pixel-based Classification

Hyperion results exhibited recognizable pattern of GV, NPV, shadow, soil, agricultural land, and impervious (Figure 3). In this figure, areas mapped as red (NPV) are considered the highest fire danger because of an abundance of senesced plant material. The fuel type map in Figure 4 was obtained using SMA result (Figure 3). All main classes were well recognized. However, a part of type2 class was poorly classified because agricultural land had similar to NPV in the spring season.

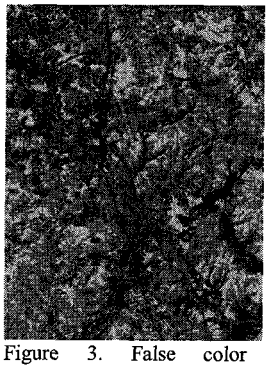

Figure 3. False color composite(pixel) showing fraction images for NPV(red), GV(green), and soil(blue)

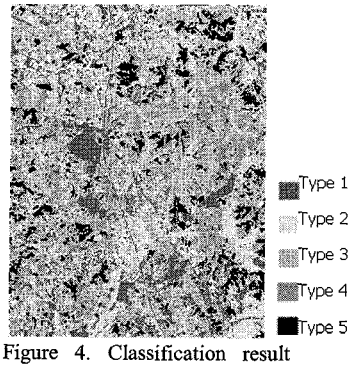


Figure 4. Classification result showing (pixel)

### 4.3 Object-oriented classification

The segmentation image in Figure 5 was produced based on optimal parameters throughout repetitive try (scale: 12; shape: 0.2; compactness: 0.7).

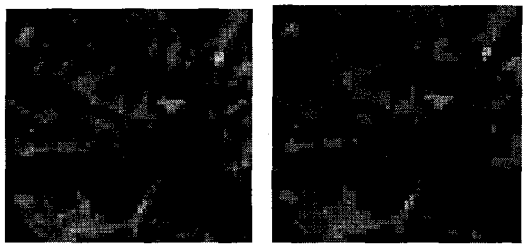

(a) Before (b) After
Figure 5. Segmentation image showing

The result of SMA also showed comparatively good performance (Figure 6), but the fraction of $SMA_{NPV}$ was relatively overestimated comparing the pixel-based SMA method. The fuel type map in Figure 7 was also obtained using SMA result (Figure 6). The fuel type map derived pixel-based SMA result showed the salt and pepper effect but the fuel type map derived object-oriented SMA result showed spectral homogenous regions.

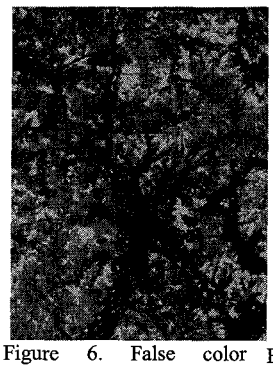

Figure 6. False color composite(object) showing fraction images for NPV(red), GV(green), and soil(blue)

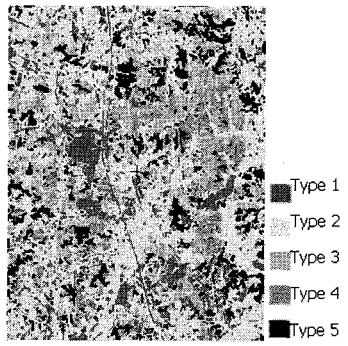


Figure 7. Classification result showing (object)

### 4.4 Validation

The results of object-oriented and pixel-based classifications were validated by comparing the true-color high resolution orthoimagery. From the results of

Table 1. Summary of confusion matrices for the accuracy of object-oriented and pixel-based classifications

| | Object-oriented classification | | Pixel-based classification | |
|---|---|---|---|---|
| | Producer(%) | User(%) | Producer(%) | User(%) |
| Type1 | 93.18 | 100.00 | 93.18 | 98.80 |
| Type2 | 96.94 | 91.35 | 73.47 | 82.76 |
| Type3 | 38.18 | 77.78 | 47.22 | 51.52 |
| Type4 | 91.78 | 49.63 | 70.67 | 49.07 |
| Type5 | 91.74 | 97.09 | 88.07 | 95.05 |
| Overall accuracy = 80.75% | | | Overall accuracy = 74.06% | |
| $K_{hat}$ = 76.11% | | | $K_{hat}$ = 67.58% | |

the confusion matrices, the overall accuracy of the object-oriented classification was better than for the pixel-based classification, 80.75% versus 74.06% respectively (Table 1). This was also the case for the $K_{hat}$. The class that had poor accuracy in both classifications were Type3 and Type4. This is possibly due to ambiguous divisions for each class.

## 5. CONCLUSION

Hyperspectral data such as Hyperion imagery provides a variety of wildfire fuel properties including in-direct measures of live fuel moisture and green live biomass, improved separation of GV, NPV and substrate and improved fuel type mapping. In this paper, we analyzed and compared object-oriented and pixel-based classification methods for fuel type mapping. The object-oriented method use in this paper provided results with an acceptable accuracy better than the pixel-based classifications. The difference between the classifications is obvious. Even though pixel-based classification is still successful, it does misclassify pixels, particularly in fuel types that are spectrally heterogeneous. Object-oriented classification appeared to overcome some of the problems encountered using pixel-based method. To improve the accuracies of the object-oriented classification, further work refining the process is continuing.

## REFERENCES


References from Journals:

Chuvieco, E., and Salas, J., 1996. Mapping the spatial distribution of forest fire danger using GIS. *International Journal of GIS*, 10(3), pp. 333-345

Dennision, P. E., Robers, D. A., and Regelbrugge, J. C., 2000. Characterizing chaparral fuels using combined hyperspectral and synthetic aperture radar data. *In Proc. 9th AVIRIS Earth Science Workshop*, 6, pp. 119-124

Han, T., Goodenough D. G., Dyk, A., and Love, L., 2002, Detection and correction of abnormal pixels in hyperion images, ?

Keane R. E, Burgan, R., and Watendon, J., 2001. Mapping wildland fuels for management across multiple scales: Integrating remote sensing, GIS, and biophysical modeling. *International Journal of Wildland Fire*, 10, pp.301-309

Kettig, R.L. and Landgrebe, D.A., 1976. Classification of multispectral image data by extraction and classification of homogeneous objects, *IEEE Transaction on Geoscience Electronics*, 14(1), pp.19-26

Roberts, D. A. and Dennision, P. E., 1999. Hyperspectral technologies for wildfire fuel mapping. *in Proc. 4th Int. Workshop on RS and GIS Applications to Forest Fire Management*, pp. 66-75

Roberts, D. A., Dennison, P. E., Gardner, M. E., Hetzel, Y., Ustin, S. L., and Lee C. T., 2003. Evaluation of the potential of hyperion for fire danger assessment by comparison to the airborne visible/infrared imagine spectrometer. *IEEE Transaction Geoscience Electronics*, 41(6), PP.1297-1310

Smith, M. O., Ustin, S. L., Adams, J. B. and Gillespie, A. R., 1990. Vegetation in deserts: I. A regional measure of abundance from multispectral images. *Remote Sensing of Environment*, 31, pp. 1-26

Tueller, P.T., 1987. Remote sensing science applications in arid environments. *Remote Sensing of Environment*, 23, pp. 143-154

Tompkins, S., Mustard, J. F., Pieters, C. M., and Forsyth D. W., Optimization of endmembers for spectral mixture analysis. . *Remote Sensing of Environment*, 59, pp. 472-489

van der Sande, C.J., S.M. de Jong, and A.P.J. de Roo, 2003. A segmentation and classification approach of IKONOS-2 imagery for land cover mapping to assist flood risk and flood damage assessment, *Internationa. Journal of Applied Earth Observation and Geoinformation*, 4, pp.217-229.

Xiao, J. and Moody, A., 2005. A comparison of methods for estimating fractional green vegetation cover within a desert-to-upland transition zone in central New Mexico, USA, . *Remote Sensing of Environment*, 98, pp. 237-250